



1 **Changes in tropical cyclone-associated precipitation of highly** 2 **damaging Philippine typhoons using high-resolution PGW** 3 **simulations and multiple-experiment approach**

4 Rafaela Jane Delfino^{1,2,3*}; Gerry Bagtasa^{1,3}; Pier Luigi Vidale^{2,4}; Kevin Hodges^{2,4}

5

6 ¹ Institute of Environmental Science & Meteorology, University of the Philippines - Diliman, Quezon City,
7 Philippines

8 ² Department of Meteorology, University of Reading, Reading, United Kingdom

9 ³ Natural Science Research Institute, University of the Philippines - Diliman, Quezon City, Philippines

10 ⁴ National Center for Atmospheric Sciences, Reading, United Kingdom

11

12 * Correspondence to: Rafala Jane Delfino (rdelfino@iesm.upd.edu.ph)

13 ORCID ID: Rafaela Jane Delfino [0000-0001-8612-0342](https://orcid.org/0000-0001-8612-0342); Pier Luigi Vidale [0000-0002-1800-8460](https://orcid.org/0000-0002-1800-8460); Gerry Bagtasa
14 [0000-0002-5433-7122](https://orcid.org/0000-0002-5433-7122)

15

16 **Abstract.** This study has investigated the changes in tropical cyclone (TC)-associated precipitation in the
17 Philippines under past (pre-industrial) and future climate scenarios using the pseudo-global warming technique
18 and dynamical downscaling. What is novel in this work is the use of high-resolution PGW simulations (3km and
19 5km) and a multiple-experiment approach to directly quantify TC precipitation changes over the Philippines,
20 revealing the nonlinear response of precipitation scaling to different warming pathways. Future climate
21 simulations project a significant increase in TC precipitation, consistent with Clausius-Clapeyron (CC) scaling
22 expectations. However, small deviations from this expected scaling are noted, attributed to factors such as
23 increased TC intensity and atmospheric warming. The simulated TC precipitation in the past climate is found to
24 be lower than that in the current climate. Our convection-permitting model experiments estimate that the average
25 TC inner-core precipitation rate changes from past to current climate conditions are 6% and 8% for the 5km and
26 3km, respectively. Under the SSP5-8.5 future scenario, simulations indicate a robust rise (by approximately 6%
27 per 1K increase in SST relative to the current climate) in the mean precipitation rates for intense TCs such as
28 Haiyan (2013), Bopha (2012), and Mangkhut (2018) in both the 5km and 3km experiments. Notably, simulations
29 that warm only land and sea surfaces show increases exceeding CC expectations, reaching up to 13% per 1K
30 increase in SST. Increases in both radial and vertical extent of rain are observed. Our analysis shows that these
31 changes are linked to enhanced latent heating, moisture, and updrafts in the TCs' inner-core regions, emphasizing
32 intricate interactions between atmospheric processes and the evolving structure of TCs. Our study underscores
33 that variations in TC intensity and structure play a crucial role in influencing the scaling relationship between sea
34 surface temperatures and TC-associated precipitation in the Philippines.

35

36 **Keywords:** tropical cyclones, precipitation, Philippines, global warming, Clausius-Clapeyron scaling



1. Introduction

38

39 Tropical cyclones (TCs) is a major source of rainfall and freshwater resources in the Philippines (Bagtasa, 2017;
40 2022; Yumul *et al.*, 2012). In some regions, over half of the annual rainfall is associated with TC-induced
41 precipitation (Bagtasa, 2017; Kubota and Wang, 2009). Projected warming is expected to intensify tropical
42 cyclone rainfall, raising risks of flooding and landslides (Knutson *et al.*, 2021; Liu *et al.*, 2019; Kossin, 2018).

43

44 A common reference is the Clausius–Clapeyron (CC) scaling, which suggests about 7% more atmospheric
45 moisture per degree of warming, enhancing rainfall potential. (Trenberth *et al.*, 2007; Allen & Ingram, 2002; Held
46 & Soden, 2006). The IPCC AR6 concludes that average TC rainfall rates are very likely to increase with continued
47 warming, and that peak rainfall rates may surpass CCS scaling in certain regions. A multi-model study by Knutson
48 *et al.* (2020) projected a global increase in TC rainfall of +6% to +22% under a +2°C warming scenario. In the
49 Western North Pacific (WNP), reported increases consistently fall within +5% to +7% per °C (Wang *et al.*, 2014;
50 2015). Similarly, the ESCAP/WMO Typhoon Committee assessment (Cha *et al.*, 2020) estimated a median rise
51 of 17% in TC precipitation rates for the WNP, with a 10th–90th percentile range spanning +6% to +24%. However,
52 TC-associated precipitation may increase at higher rates per degree change in temperature due to dynamic
53 processes, such as increased latent heat fluxes and stronger convergence, which amplify rainfall beyond the
54 thermodynamic expectations (Shi *et al.*, 2024). Empirical studies have supported the application of CCS in
55 explaining increases in TC precipitation (Trenberth *et al.*, 2007; Vecchi *et al.*, 2008). Nonetheless, regional
56 discrepancies have been observed. Kossin *et al.* (2017) and O’Gorman (2020) noted that observed precipitation
57 changes in certain regions deviate from CCS, likely due to TC dynamics, moisture transport, and local atmospheric
58 circulation.

59

60 Recent literature describes Super-CCS, where rainfall rises faster than the 7% per °C benchmark. For example,
61 Liu *et al.* (2019) and Huprikar *et al.* (2024) documented inner-core rainfall increases beyond CC expectations,
62 linked to eyewall expansion and stronger updrafts. Liu *et al.* (2019) reported that rainfall rates within a 100-km
63 radius from the center for TCs with tropical storm intensity could increase by 13%–17% per °C under 21st-century
64 warming. Huprikar *et al.* (2024) also found that future rainfall associated with Hurricane Irma exceeded CCS
65 expectations. These findings suggest that TC inner-core intensification and structural changes, such as vertical
66 expansion of the eyewall and enhanced updraft, play a critical role in amplifying precipitation beyond the CCS
67 rate.

68

69 Despite these findings, there is still a limited understanding of whether TC-associated rainfall in the Philippines
70 conforms to CCS or exhibits Super-CCS properties, especially under changing climate conditions where TCs are
71 projected to intensify (Delfino *et al.*, 2023; 2024). While previous studies have examined TC intensity and
72 precipitation changes (Villarini *et al.*, 2014; Patricola & Wehner, 2018; Liu *et al.*, 2019; Xi *et al.*, 2023), detailed
73 analyses that isolate rainfall scaling with warming remain sparse. Unlike previous case-specific studies, this work
74 systematically applies the PGW framework to multiple Philippine landfalling TCs across three climate states (pre-
75 industrial, present, and future). This study hopes to provide additional evidence of how warming will intensify
76 landfall rainfall hazards in the Philippines. Specifically, we investigate the following:



- 77 • How does the TC-associated precipitation in the Philippines change under past and future climate
78 scenarios, and to what extent do these changes align with the expectations of CCS?
79 • How do variations in TC intensity and structure influence the scaling relationship between sea surface
80 temperatures and TC-associated precipitation in the Philippines?

81

82 A better understanding of these mechanisms is critical for anticipating current and future flood risks and improving
83 disaster preparedness in the Philippines. Section 2 of this paper discusses the methods, Section 3 provides the
84 results and discussion, and Section 4 highlights the conclusions.

85

86 2. Methods

87

88 2.1 Model Configuration

89

90 We used WRF-ARW v3.8.1 (Skamarock et al., 2008) with two main setups: (i) a nested 25 km–5 km grid with
91 cumulus parameterization and (ii) a convection-permitting single 3 km grid without cumulus parameterization.
92 Both applied 44 vertical levels from surface to 50 hPa. Further physics choices and TC tracking follow Delfino et
93 al. (2023).

94 2.2 Experimental Design

95

96 Three TC cases are selected based on the region in the Philippines where the TCs made landfall, the month of
97 occurrence, and associated damages – Typhoons Haiyan (2013), Bopha (2012), and Mangkut (2018). More
98 detailed information on these three TC cases is described in Delfino et al. (2023). The three TC cases were
99 simulated with four different initialization times (00, 06, 12, and 18 UTC) to create an ensemble from a single
100 driving reanalysis, thereby minimizing uncertainties from variations in the initial conditions. For tracking the
101 simulated TCs, the simulated track and intensity values were obtained every 6 hours using the TRACK algorithm
102 (Hodges et al., 2017) as used in Hodges and Klingaman (2019) and Delfino et al. (2023).

103

104 Multi-model datasets from the Coupled Model Intercomparison Project phase 6 (CMIP6) were used to apply the
105 Pseudo-Global Warming (PGW) method. We simulated the three TC cases under different climate conditions by
106 primarily adjusting the following parameters: SST, atmospheric temperature, and relative humidity (RH) between
107 current, pre-industrial, and future climate conditions. Four CMIP6 models were used, and results for all ensemble
108 members were averaged for each of the CMIP6 models. The models - HadGEM3-C31-LL, CESM2, MIROC6,
109 MPI-ESM1-2-HR – were chosen to represent different warming levels, under the Shared Socio-economic
110 Pathways (SSP) 5-8.5 scenario. Monthly mean deltas from CMIP6 (2070–2099 minus historical) were applied to
111 ERA5 boundary and initial fields. Three experiment sets were tested: (1) SST-only (SFC), (2) SST plus
112 tropospheric temperature (SFC+PLEV), and (3) SST, temperature, and humidity (FULL). Each case was
113 simulated with four initialization times to form ensembles. A more detailed description of the methodology can
114 be found in Delfino et al. (2023).

115

116



It is also important to note here that the PGW technique faces challenges related to spin-up and dynamical balance when simulating TCs. Spin-up issues arise because the initial conditions need time to adjust to imposed future climate anomalies, potentially leading to unrealistic results during the adjustment period. Additionally, altering these conditions can disrupt the dynamic balance of the atmospheric system, resulting in inaccuracies in the intensity and behavior of simulated TCs. These issues were explored and addressed in Delfino et al., (2024).

2.3 TC precipitation analysis

Rainfall analysis included hourly rates, accumulated totals, and reflectivity composites during peak intensity. The forward sector of each storm was emphasized, as this region typically hosts the strongest convection due to storm motion combined with cyclonic rotation. We also investigated the relationships between TC rain rate and TC wind speed, emphasizing how this relationship varies within the TC inner-core region (2.5° distance from the center). We also analysed the simulated reflectivity rates (in dbz) from the WRF simulations and vertical profiles of the averaged composites over multiple time steps (e.g., average reflectivity during peak intensity hours) of simulated reflectivity over a 2.5° radius in the forward direction of the storms for the simulations, since TCs typically have the highest precipitation rates and strongest reflectivity in their forward quadrant due to the combined effects of TC motion and cyclonic rotation. By focusing on this region, we can capture the most intense precipitation features and better understand the TC's impact. Reflectivity is particularly useful because it provides insight into the microphysical structure of convection within TCs. Higher reflectivity values typically correspond to deeper and more intense convective cores, which are closely linked to strong updrafts and heavy rainfall production. The profiling is done at peak intensity at height levels between 0 and 18 km, and the radial grid extends to 10° for each simulation.

3. Results and Discussion

3.1 Changes in the total accumulated rainfall

The discussions in Sections 3.1 and 3.2 below are from the FULL experiments, with additional discussions on other sets of experiments in Section 3.3. In the FULL experiments, rainfall consistently increased under future warming compared with the present, while simulations under pre-industrial conditions produced less precipitation. This progression highlights stronger rainfall across pre-industrial, present-day, and future climates. Future precipitation changes in the FULL experiments reached a maximum percentage change in hourly rainfall rate of 18% (18%) for Haiyan, 11% (20%) for Bopha, and 26% (7%) for Mangkhut in the 5kmCU (3kmNoCU) runs under future climate conditions; and up to more than 18% (18%) in total accumulated precipitation over the simulation period for Typhoon Haiyan, 12% (20%) for Bopha, and 25% (7%) for Mangkhut (Figure 1). In contrast, in the simulations under pre-industrial climate conditions, TC-associated precipitation are less than the current climate, with percentage changes (pre-industrial minus current) in total accumulated precipitation over the simulation period of -3%(-2%) for Haiyan, -20%(0%) for Bopha, and -6%(-16%) for Mangkhut; and percentage



change in precipitation rate of -3%(-2%) for Haiyan, -19%(0%) for Bopha, and -2%(-16%) for Mangkhut in the 5kmCU(3kmNoCU) runs (Figure 1).

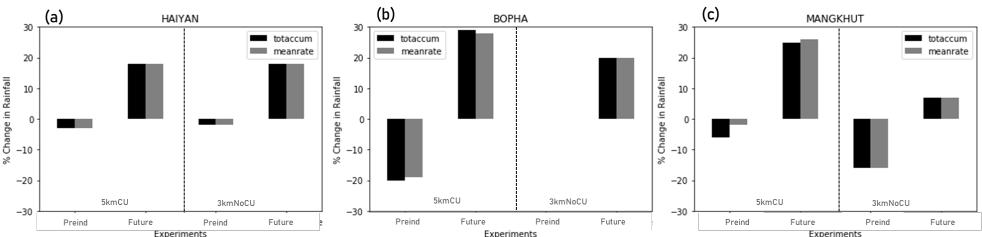


Figure 1. Percent changes in total accumulated and mean precipitation rate relative to current climate for the 5kmCU runs (left panel) and the 3kmNoCU runs (right panel) under the pre-industrial and future climate relative to current climate conditions for (a) Typhoon Haiyan, (b) Typhoon Bopha, and (c) Typhoon Mangkhut

Examination of the time series of accumulated precipitation, together with variations in RH, shows that precipitation under the future climate generally exceeds that of the current climate, while the current climate also produces greater TC rainfall than the pre-industrial period across both variables (Figure 2). Under future climate conditions, accumulated precipitation consistently and markedly increases relative to the current climate, suggesting the likelihood of more intense and prolonged precipitation episodes. . Similarly, the current climate model runs exhibit higher accumulated precipitation than those of the pre-industrial period, reflecting an ongoing trend of changing precipitation patterns over time. Simultaneously, changes in RH are scrutinized in conjunction with the accumulated precipitation. The analysis reveals the same upward trajectory, with higher RH levels (Figure 2, right panels) in both the current and future climates compared to the pre-industrial era.

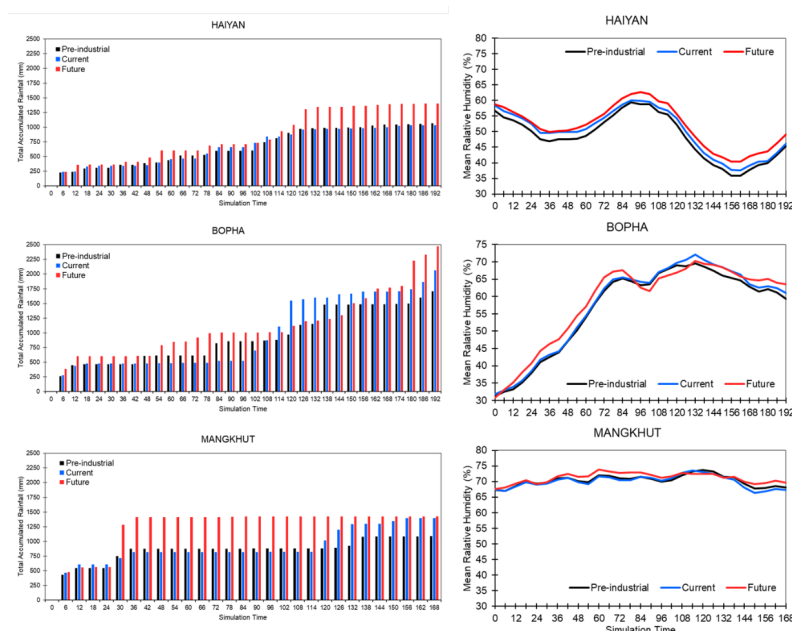


Figure 2. Total accumulated precipitation (left panel) and mean mid-tropospheric RH (right panel) of the TC cases under pre-industrial, current, and future climate throughout the simulation period of the three TC cases under the 5kmCU simulations.

Figure 3 presents the differences in total accumulated rainfall between Current minus Pre-industrial (upper panels) and Future minus Current (lower panels). In Figure 3a, a statistically significant overall increase ($p = 0.0066$) is evident, particularly across the central Philippines. For Bopha, moderate increases are observed over parts of Mindanao and the Visayas, with a mean significant rise of 1.7%. Mangkhut, by contrast, displays a pronounced increase in total accumulated rainfall, most notably over northern Luzon, with a mean rise of 14.2 mm (10.5%), highly significant at $p < 0.0001$. In the Future minus Current climate comparisons, Haiyan shows a marked increase in rainfall across the Visayas and central Mindanao, with a mean increase of 10.1 mm (7.4%), also statistically significant. Bopha shows the largest increase, especially over Luzon and the Visayas, with an average rise of 26.3 mm (24.3%). Mangkhut, however, exhibits only a minimal increase in rainfall over northern Luzon and adjacent regions, with a mean increase of 3.9%, largely attributable to a slight northward displacement of its track in the future climate simulations.

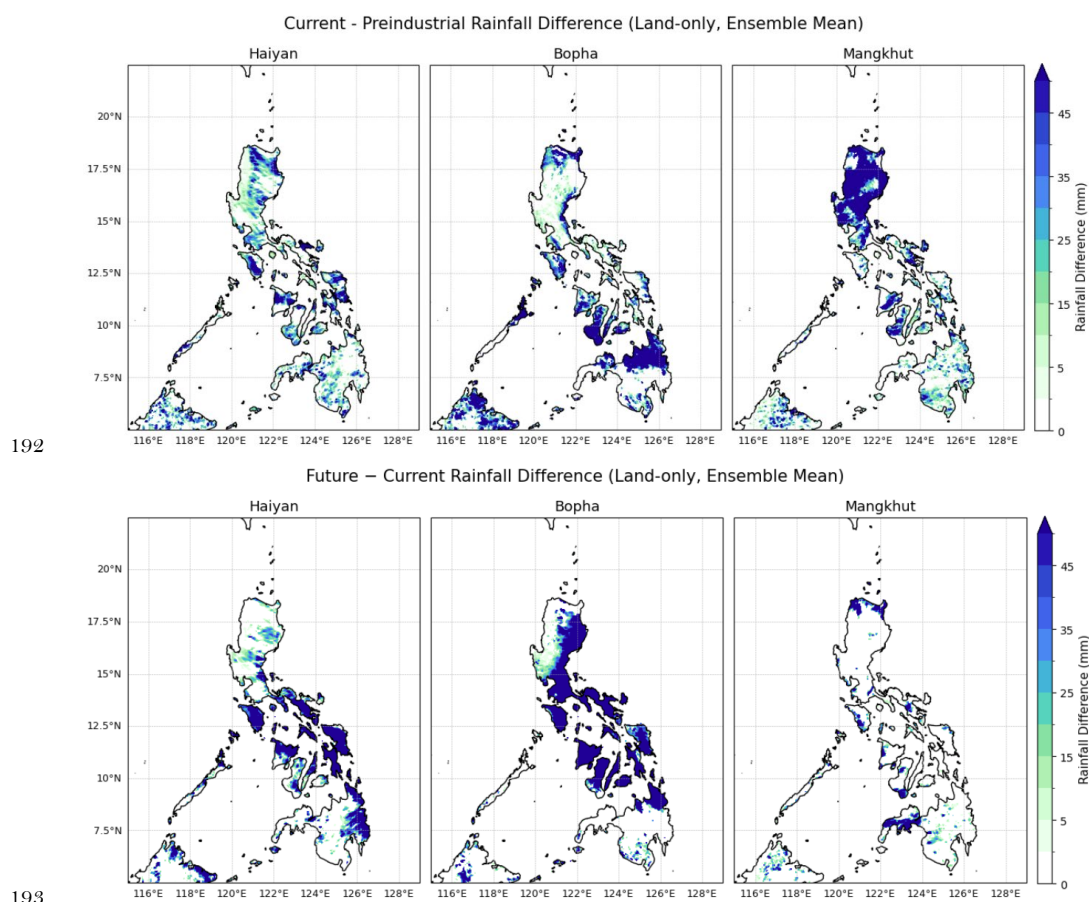


Figure 3. Difference in the ensemble-mean accumulated precipitation (a-c, top panels) Current minus Pre-industrial; (d-f, bottom panels) Future minus Current for Typhoons Haiyan (left), Bopha (middle) and Mangkhut (right) under the 3kmNoCU simulations.

Figure 4 shows the boxplots of the distribution of total accumulated rainfall (in mm) for the three typhoons under the three climate scenarios: Preindustrial (black), Current (blue), and Future (red). This shows that both Haiyan and Bopha exhibit substantial increases in total rainfall with warming, whereas Mangkhut shows a relatively smaller increase. For Typhoon Haiyan, the ensemble median total rainfall increases in the Future scenario by approximately 9% increase. For Bopha, we are looking at approximately 23% increase from preindustrial to the future scenario, while Mangkhut exhibits minimal change. The interquartile range (IQR) also shifts upward, with higher ensemble spread under future warming for all three TCs, again with relatively minimal change for Mangkhut compared to Haiyan and Bopha. The current scenario shows little deviation from preindustrial.

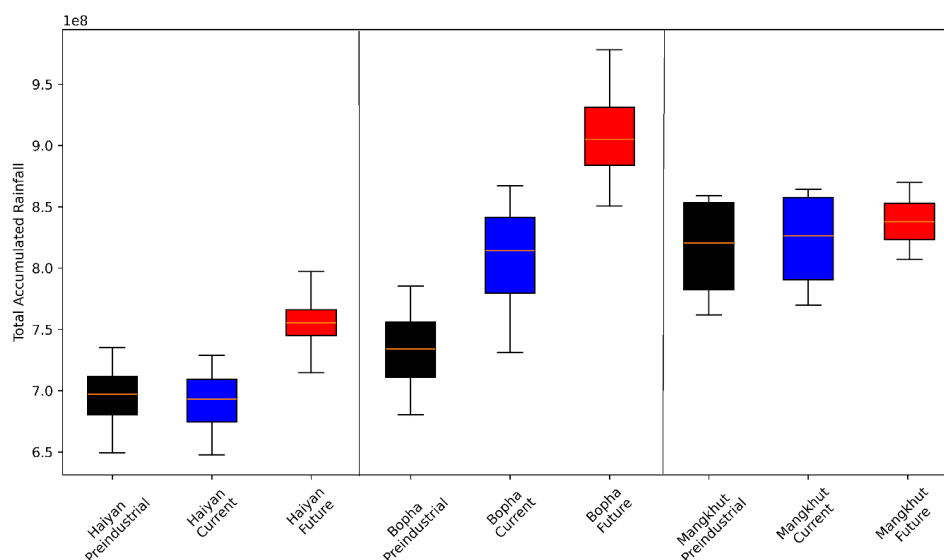
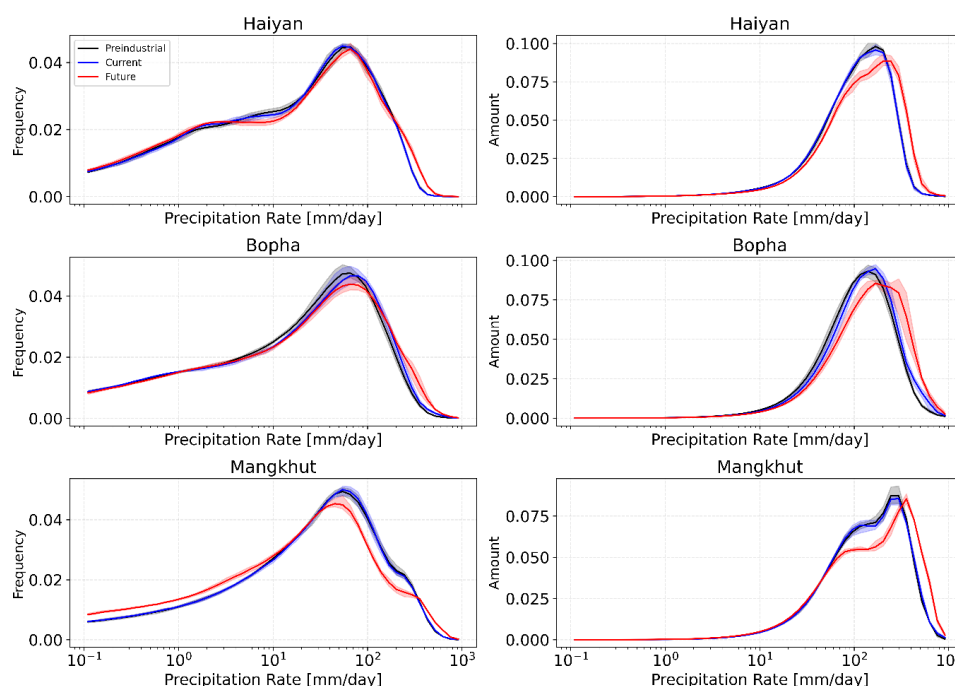


Figure 4. Boxplots for the Total Accumulated Rainfall within a 2.5° radius of the center of the track from the preindustrial, current, and future climate scenarios for Typhoons Haiyan, Bopha, and Mangkhut under the 3kmNoCU simulations using all ensemble members.

3.2 Changes in TC rain rate and intensity in the simulations

Figure 5 below shows the frequency distributions of the rainfall rates for Haiyan, Bopha, and Mangkhut across three climate scenarios (Preindustrial, Current, Future), with the left panels showing the frequency of different precipitation rates (in mm/day) and the right panels showing the distributions of the rainfall amount associated with each precipitation rate. Based on this figure, the future scenarios (red line) show a rightward extension (tail), indicating an increase in the frequency of higher rates across all TCs. Meanwhile, most total rainfall amounts (right panels) in current and future climates are in the higher end (≥ 100 mm/day).



221

222 **Figure 5. Distributions of Typhoons Haiyan, Bopha, and Mangkhut's precipitation rate (left panels),**
 223 **frequencies (%), and (right panels) amounts (mm d-1) for the pre-industrial, current, and future scenarios**
 224 **under the 3kmNoCU simulations using all ensemble members.**

225

226 Figure 6 shows the boxplots of percent changes in mean, 95th, and 99th percentiles of 6-hourly rainfall rates for
 227 Haiyan, Bopha, and Mangkhut relative to the current climate scenario. Future simulations (red boxes) show
 228 consistently higher median percent increases, particularly for the mean rainfall across all TCs. However, the
 229 rainfall extremes (95th and 99th percentiles) increase more modestly, but in most cases, they still exceed the 7%/K
 230 baseline, suggesting potential influence from TC intensity. The figure also shows a high spread in the ensemble
 231 in terms of spread and outliers, particularly in the percent changes in mean rainfall.

232

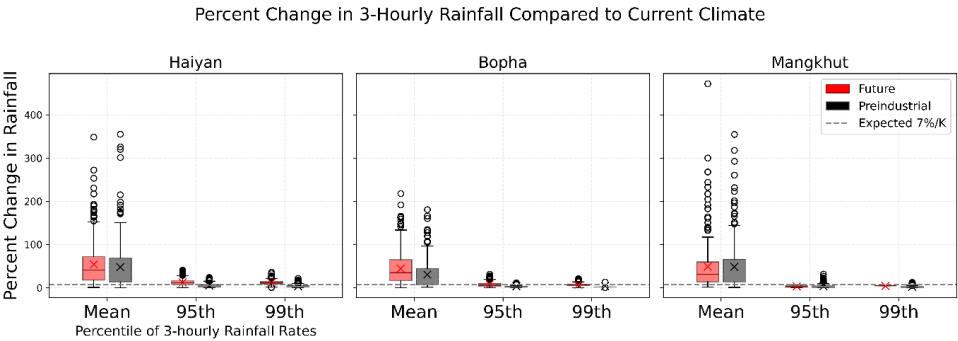


Figure 6. Percent change in 6-Hourly Rainfall Rates of the Pre-industrial and Future simulations compared to Current simulations for Typhoons Haiyan, Bopha, and Mangkhut. The x-axis shows different metrics: mean 6-hourly rate, and 95th and 99th percentiles. The X markers denote the average percent change, and the black

A recent study by Macalalad et al. (2023) investigated the effects of historical warming on a different TC case, Typhoon Vamco (2020), and found that the influence of historical warming are counteracted by additional factors such as orography and topography, resulting in comparable precipitation levels between past and present simulations within two river basins in the Philippines. To isolate the topographic effects of TC-associated precipitation, we analysed the TC precipitation rate at the time the simulated TCs reached peak intensity prior to landfall. In the 3kmNoCU experiments, the percent change in average rain rate for Future minus Current (and Current minus Pre-industrial) is 10% (1%) for Typhoon Haiyan, 13% (10%) for Typhoon Bopha, and 9% (14%) for Typhoon Mangkhut. In the 5kmCU experiments, the corresponding percent changes are 17% (1%) for Haiyan, 11% (13%) for Bopha, and 14% (5%) for Mangkhut. Increases in precipitation are concentrated in the inner-core regions of the TCs (Figures 7, 8, and 9 for Haiyan, Bopha, and Mangkhut, respectively), with the signal more pronounced in the 5kmCU simulations. In the 3kmNoCU simulations, there are coherent spatial patterns in the future precipitation response characterized by drying in the outer core, resulting in precipitation responses that are stronger over the inner core region in all three TC cases. This drying outer core condition is also present in the 5kmCU future run for Mangkhut. Such drying has also been found by Patricola and Wehner (2018), particularly in the weaker TCs.

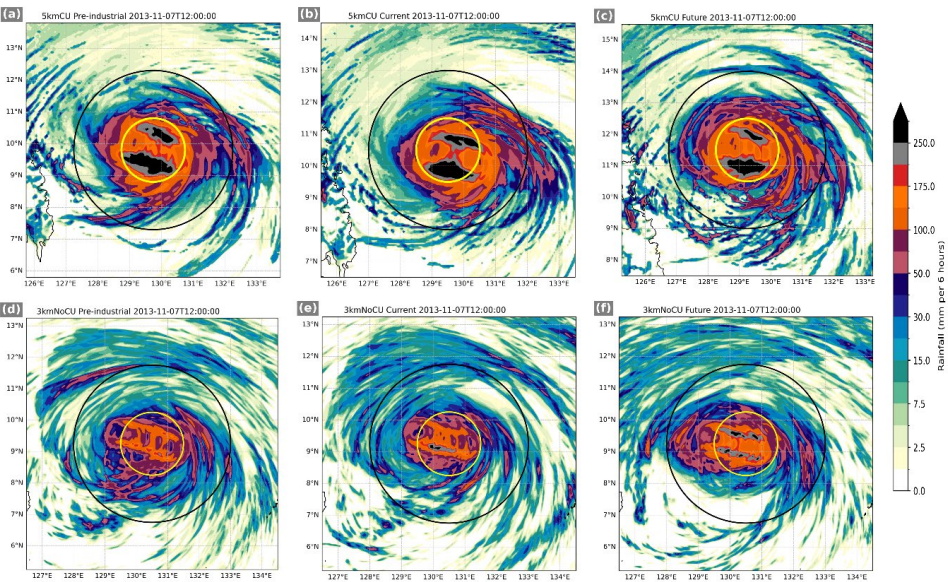


Figure 7. Simulated precipitation rate (mm/hr) at simulated peak intensity for Haiyan on 7 November 2013 12UTC for the 5kmCU runs (upper panel) and the 3kmNoCU runs (lower panel) under the pre-industrial (left), current (middle), and future climate conditions. The black circle indicates the 2.5° radius from the center, and the yellow circle indicates the 1° radius from the center.

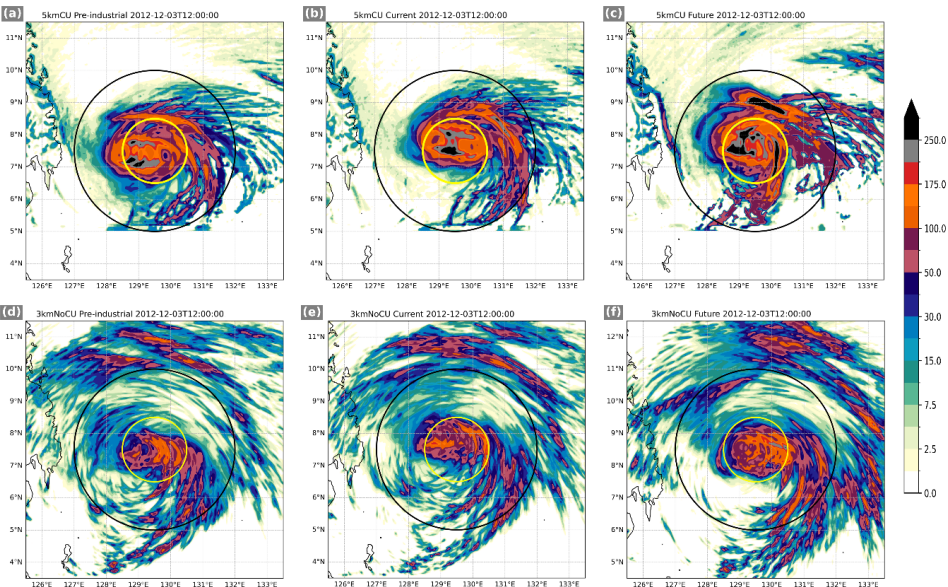


Figure 8. Same as Figure 7, but for Bopha

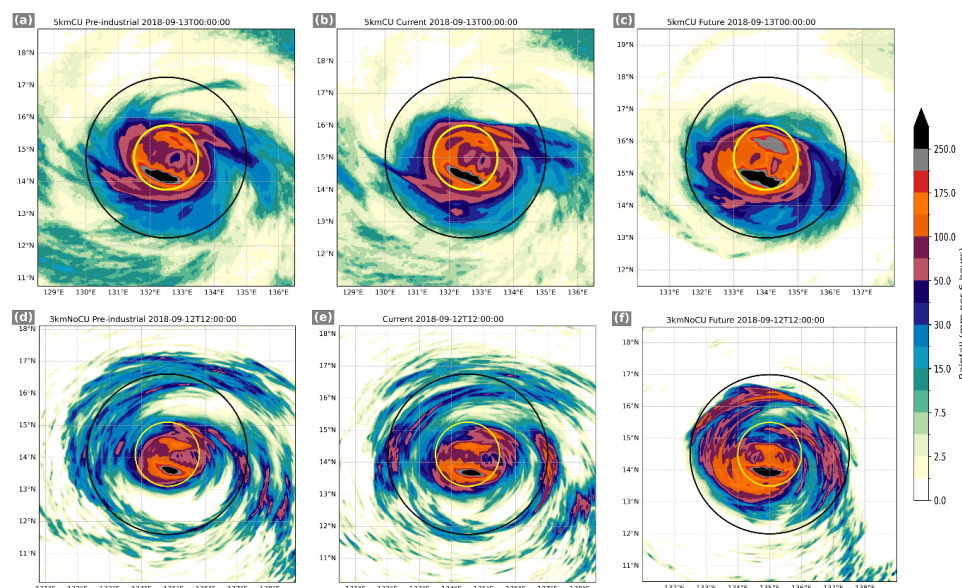


Figure 9. Same as Figure 7, but for Mangkhut

3.3 Changes in TC rain rate and Clausius-Clapeyron scaling

According to Liu *et al.* (2019), a projected increase in precipitation rate that is more than what is expected according to the CCS relation may be linked to enhanced TC intensity associated with land surface and SST warming. As shown in Figure 10a, the largest increases in precipitation tend to occur when only the surface temperatures have been warmed (SFC only). In contrast, a lower increase is found when atmospheric warming is also included (SFC+PLEV) and RH changes (FULL). In the SFC-only simulations, future precipitation changes exceed 17% per degree of SST warming, surpassing the CCS rate..

By comparison, both the 5kmCU and 3kmNoCU simulations with varying initializations (Figure 10b) remain within this thermodynamic expectation under future climate conditions. Likewise, the change in rain rate relative to the pre-industrial climate is consistently within the CCS for all typhoons (not shown). These results are consistent with Stansfield and Reed (2023), who found that the apparent scaling of TC precipitation in response to SST warming is typically around 6–9% per K, consistent with the CCS rate, while the climate scaling - which accounts for long-term climate changes - is smaller, around 5% per K. They emphasized that the apparent scaling reflects short-term changes driven by SST alone, while climate scaling incorporates broader atmospheric changes like shifts in wind shear, which reduce the precipitation intensification seen in the SFC-only experiments of Liu *et al.* (2019).

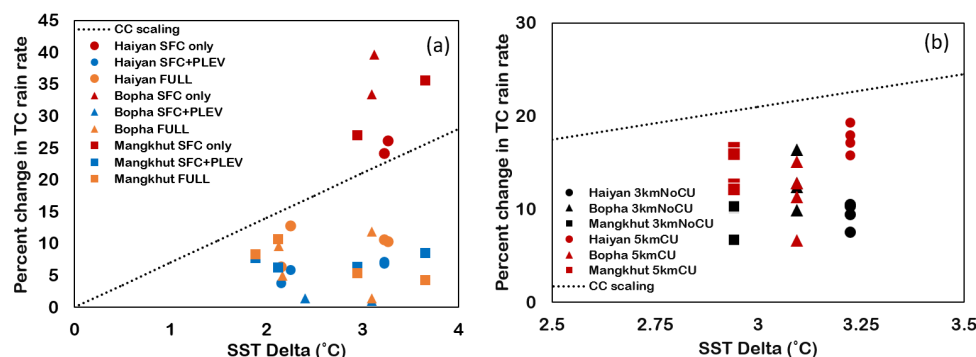


Figure 10. Percentage change in TC inner core rain rates vis-à-vis SST delta. (a) 5kmCU simulations using different levels of PGW delta and (b) 5kmCU and 3kmNoCU simulations using different initializations. The black dotted lines show the Clausius-Clapeyron scaling.

Figure 11 shows the relationship between simulated TC intensity and inner-core precipitation rates from the 5kmCU and 3kmNoCU experiments. In the present-climate simulations, TC intensity and inner-core rain rate exhibit an approximately linear relationship, with a regression slope of $0.807 \text{ (mm h}^{-1}) \text{ per (m s}^{-1})$ (Figure 11a). Under future and pre-industrial climate conditions, both the 5kmCU and 3kmNoCU experiments yield a similar relationship, though with a lower regression slope of $0.38 \text{ (mm h}^{-1}) \text{ per (m s}^{-1})$ (Figure 11b). Overall, inner-core rain rate is positively correlated with TC intensity: in the 5kmCU simulations, a 1 m s^{-1} increase in TC intensity corresponds to a $\sim 1.17 \text{ mm h}^{-1}$ increase in rain rate, while in the 3kmNoCU simulations the increase averages $\sim 0.66 \text{ mm h}^{-1}$. Considering the sensitivity of TC intensity to SST and the dependence of rain rate on intensity, we further examined the sensitivity of TC precipitation to SST. Our findings indicate that the TC inner-core rain rate of the three TC cases (for both 3kmNoCU and 5kmCU runs) will increase by approximately 6% per 1 K increase in SST in the future. This increase can be understood through the combined effects of TC intensity sensitivity to SST and CCS. However, larger increases (up to 33% per 1K increase in SST) can be found in the 5kmCU SFC-only experiments, which may be due to the changes in thermodynamics and shifts in TC trajectory (Delfino et al., 2023). The rest of the simulations under the 5kmCU SFC+PLEV and FULL and 3kmNoCU experiments show no significant changes in track.

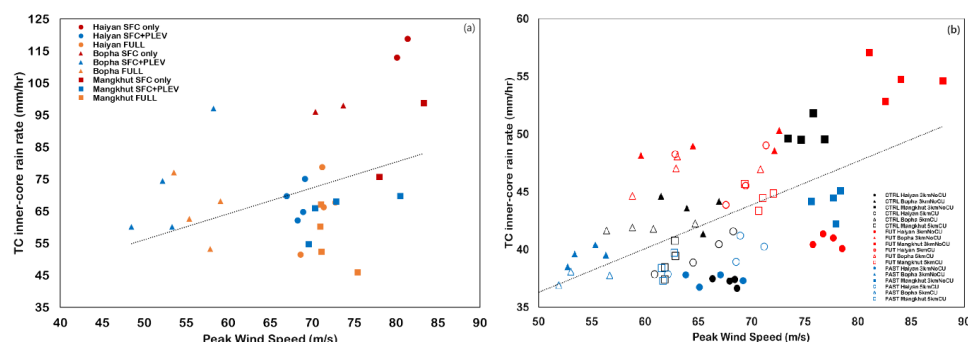


Figure 11. Dependence of TC inner-core rain rate on TC intensity. (a) 5kmCU simulations using different levels of PGW delta and (b) 5kmCU and 3kmNoCU simulations using different initializations.

3.4 Potential mechanisms driving TC-associated precipitation changes

Figure 12 presents the vertical profiles of the averaged composites of simulated reflectivity within a 2.5° radius in the forward direction of the typhoons for the 3kmNoCU simulations, the 5kmCU simulations exhibit similar patterns (not shown). The composites are taken at peak intensity across different height levels between the surface up to 18 km. Results indicates substantial increases in simulated reflectivity throughout the vertical column, particularly within the TC's primary circulation. This in turn, leads to deeper core convection in the future climate simulations, as seen in the upward extension expansion of the eyewall.

The vertical expansion of the eyewall, the inner region of TC with intense convection and strongest winds surrounding the eye of the storm, is consistent with what is found in the vertical cross-section of the composite of azimuthally averaged winds (Delfino et al., 2023). As indicated by the increased reflectivity observed in Figure 12, this provides insights into the evolving structure of TCs under the different climate conditions simulated in the study. Although the composites are taken at the peak intensity of the TCs, the results reveal substantial enhancements in reflectivity throughout the vertical extent within a 2.5° radius around the TC's forward direction. This enhanced reflectivity suggests a greater amount of precipitation within the TC's inner core, which has implications for its overall dynamics. The explanation for the vertical expansion of the eyewall lies in the interactions between different atmospheric processes. As TC intensity increases, precipitation rates within the storm also tend to increase (Alvey et al., 2015), reflecting and reinforcing internal dynamical processes critical to intensification. Although warm sea surface temperatures, weak vertical wind shear, and high low-level moisture are recognized as necessary environmental conditions for TC development (DeMaria et al., 2005; Kaplan et al., 2010, 2015), these factors alone are insufficient to account for observed variations in TC intensity (Hendricks et al., 2010). This has led to a growing focus on internal TC processes, particularly precipitation and convection, as key drivers of TC intensification. Latent heat release from enhanced precipitation warms the TC core and contributes to further pressure falls, strengthening the cyclone (Rotunno & Emanuel, 1987; Pendergrass, 2014; Yamada, 2017). Observational studies using TRMM and passive microwave data have shown that more intense TCs are typically associated with broader and more symmetric precipitation coverage, especially in the inner core (Alvey et al., 2015). Stratiform and moderate-to-deep convective precipitation are particularly linked to rapid



intensification (Tao & Jiang, 2015), suggesting that increasing precipitation is not just a result of intensification, but a contributor to it. Ruan and Wu (2018) also found that as TCs intensify, they exhibit increased precipitation and colder high cloud tops, and that widespread very deep convective clouds (IR BT < 208 K) are strong predictors of future intensity change, particularly rapid intensification (Tierra and Bagtasa 2021).

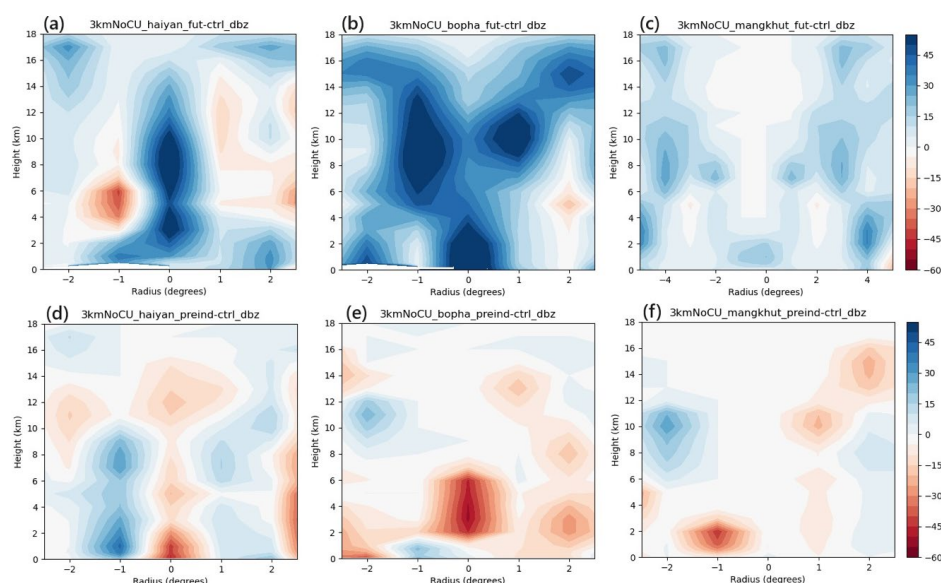


Figure 12. Radius (in degrees) – height (in km) cross sections of simulated differences in reflectivity (dBZ) from future minus current (top panels, a-c) and pre-industrial minus current (bottom panel, d-f) from the 3kmNoCU experiments. All reflectivity fields are at peak intensity while precipitation rates are shown within a $2.5^\circ \times 2.5^\circ$ grid from the center at peak intensity for Typhoon Haiyan (a and d panels), Bopha (b and e panels), and Mangkhut (c and f panels).

Vertical motion (ω) was investigated to understand the detailed processes of TC-associated precipitation intensification in different climate conditions (Figure 13). Vertical velocity fields show enhanced ascent near eyewall regions under warming scenarios, with the largest anomalies in future runs. These dynamical signals are consistent with reflectivity results, reinforcing the link between stronger updrafts and increased rainfall. Our analysis revealed significant regions of strong ascending motion, characterized by increased ω , near the eyewall and along spiral rainbands of Typhoons Haiyan, Bopha, and Mangkhut, primarily within a 250-km radius from the TC center. These regions are crucial for intense convective activity and high precipitation rates due to vigorous updrafts and condensation processes. Comparisons between future and current climate simulations reveal larger differences in ω near the TC core region, indicating a potential increase in vertical motion and precipitation rates under future climate conditions. Similarly, significant differences are also evident between current and past climate scenarios, suggesting consistent changes in vertical motion patterns over time. Our findings regarding the differences in ω between current and future climate simulations suggest a projected increase in vertical motion and moisture convergence, which will likely lead to stronger precipitation events. In



our earlier work (Delfino et al., 2023), we note that there are some changes or shifts in the vertical profiles of the TC cases that potentially led to the further intensification of rainfall associated with these TCs. Additionally, Shi et al. (2024) emphasized that TC intensification under warming is not driven solely by stronger updrafts, but also by the expansion of deep convective cores accompanied by a suppression of shallow cumulus and congestus clouds. This structural adjustment implies that while localized hourly rainfall may scale with the CCS relationship, precipitation accumulated over broader areas could increase by up to 18% per degree of warming. Understanding these dynamics is essential for predicting how TCs may evolve under different climate scenarios, particularly in terms of intensity and precipitation distribution. Overall, the study underscores the sensitivity of TC dynamics to changes in vertical motion and provides insights into the complex interactions shaping TC-associated precipitation, contributing to advancing our understanding of TC characteristics in a changing climate.

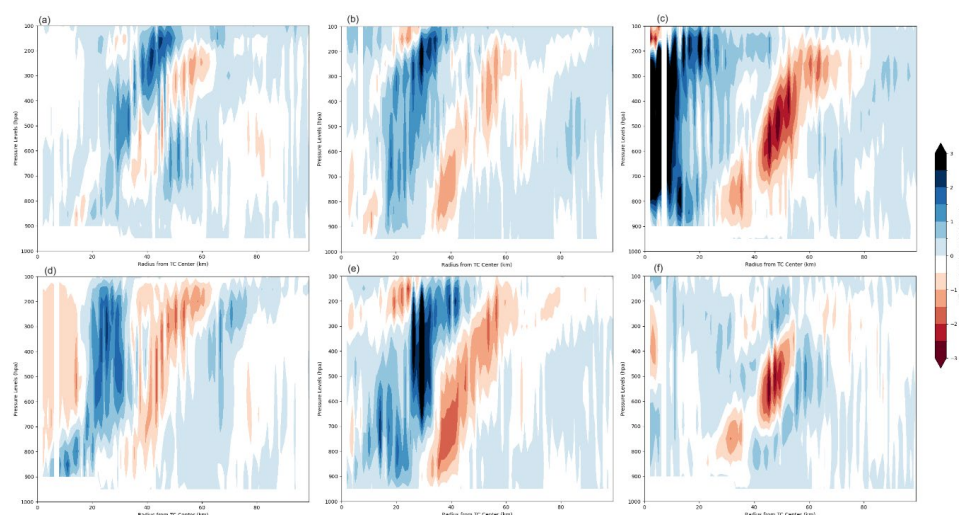


Figure 13. Simulated difference in vertical velocity, Omega (hPa s^{-1}) at several levels (1000–100hPa) within 250 km radius from the TC center for the 3kmNoCU experiments difference between future and current climate (top, a-c), and difference between current and past climate (bottom, d-f) for Typhoons Haiyan (left), Bopha (center) and Mangkhut (right).

This work advances beyond our earlier case-specific studies (Delfino et al., 2023; Delfino et al., 2024) by systematically applying the PGW framework to multiple Philippine landfalling cyclones under three climate states (pre-industrial, present, and future). By comparing rainfall scaling across storms, we demonstrate consistent Super-CC behavior in forward quadrants and highlight a progressive intensification of landfall rainfall hazards. These results provide a regional-scale perspective and connect directly to disaster risk in the Philippines, representing a new contribution beyond our previous publications.

4. Summary and conclusions



389 This study investigated the changes in tropical cyclone (TC)-associated precipitation in the Philippines under past
390 (pre-industrial) and future climate scenarios, using a hierarchy of convection-permitting simulations. Importantly,
391 this is the first time that such extreme typhoons have been systematically simulated and compared using both
392 convection-permitting and parameterised convection models. Some of the results show sensitivity to the treatment
393 of convection, while other experiments are relatively insensitive. Overall, the main findings are robust and largely
394 insensitive to this model formulation choice. In alignment with the expectations from Clausius–Clapeyron scaling
395 (CCS) for TCs, the future climate simulations project a robust increase in TC precipitation. Deviations from the
396 expected CCS scaling are attributed to factors such as increased TC intensity, also driven by atmospheric warming.

397 Under past climate conditions, TC precipitation in the Philippines would have been generally less than that of
398 current climate conditions, with an average change (current - past) in TC inner-core precipitation rates of 6% and
399 8% for the 5kmCU and 3kmNoCU experiments, respectively. The observed changes between the past and current
400 climate align with expectations from CCS, indicating that the atmosphere holds approximately 7% more water
401 vapor per degree Celsius increase in surface temperature. Conversely, under future climate scenarios, the FULL
402 simulations conducted under the SSP5-8.5 scenario indicate a robust rise - by approximately 6% per 1 K increase
403 in SST in the mean precipitation rates for specific intense TCs, such as Haiyan, Bopha, and Mangkhut, in both the
404 5kmCU and 3kmNoCU experiments, consistent with CCS expectations.

405
406 However, notable deviations from CCS arise in simulations where only the land and sea surface temperatures are
407 increased (e.g., 5kmCU SFC-only), with precipitation increases reaching up to 13% per 1 K SST increase. This
408 suggests that additional dynamical processes, such as TC track changes or structural modifications, amplify
409 precipitation beyond thermodynamic expectations. Frequency distributions of rainfall further confirmed an
410 intensification of heavy precipitation events in a warming climate. Future scenarios displayed a consistent shift
411 toward higher 6-hourly rainfall rates, particularly in the right tail (extreme values).

412
413 Notably, the results reveal an asymmetry in the response of TC precipitation between past cooling and future
414 warming. Specifically, under future warming, feedback appears to amplify precipitation (consistent with a positive
415 feedback mechanism), while in the pre-industrial simulations, these feedback act in the opposite direction,
416 dampening TC intensity and precipitation.

417
418 Spatial rainfall maps show increased precipitation from pre-industrial to present-day, and further into the future.
419 Haiyan and Bopha display substantial increases, while Mangkhut's response is comparatively modest, reflecting
420 its more northerly track. Overall, the total accumulated rainfall associated with the three TCs, within a 2.5° radius,
421 is expected to increase by up to 25% in the future.

422
423 Reflectivity profiles reveal broader and taller convective towers in warmer climates, suggesting intensified latent
424 heating and deeper storm cores, which drive more efficient rainfall production. . This is attributed to enhanced
425 latent heating, which drives stronger updrafts and contributes to a deeper TC core. Mechanistically, the deeper
426 cores lead to intensified updrafts that enhance the lift of moist air, promoting additional adiabatic warming within
427 the TC and further enhancing TC-associated precipitation. This chain of causation aligns with previous studies
428 (e.g., Yamada et al., 2017) that emphasize the role of latent heating in TC dynamics.



429

430 This study extends beyond our earlier analyses by evaluating multiple Philippine landfalling cyclones in a unified
431 PGW framework across pre-industrial, present, and future climates. The consistent emergence of Super-CC
432 scaling in forward quadrants underscores a robust intensification of rainfall hazards unique to this region. By
433 situating these findings within the Philippine disaster risk context, the study provides new insights for impact-
434 oriented assessments and highlights the need for adaptation planning to address more extreme rainfall in future
435 tropical cyclones.

436

437 Our findings provide critical insights into how variations in TC intensity and structure influence the scaling
438 relationship between SST and TC-associated precipitation in the Philippines. The heightened intensity of
439 simulated TCs under future climate conditions contributes to increased TC-associated precipitation rates within
440 the inner core, diverging from expected CCS behavior. This supports the notion of the CCS, emphasizing the
441 interplay between atmospheric moistening, TC dynamics, and evolving TC structures.

442

443 We recommend that future studies focus on (1) the climatological trends in TC precipitation i.e. effects of climate
444 change and natural climate variabilities on TC precipitation; (2) the specific impacts of changing TC tracks, the
445 role of atmospheric moisture distribution, and (3) the influence of varying SST patterns and magnitude on TC-
446 associated precipitation in the Philippines. Additionally, further research should investigate the potential effects
447 of land-use changes and urbanization on TC rainfall patterns to provide a more comprehensive understanding of
448 the local impacts of climate change on TCs.

449

450 **AUTHOR DECLARATIONS**

451

452 **Funding Information**

453

454 RJD was supported by a scholarship from the Philippine Commission on Higher Education and the British Council
455 through the JDNF Dual PhD Program. KH and PLV were funded by the UK Natural Environment Research
456 Council (NE/W009587/1). This work used the JASMIN data analysis facility (<https://www.jasmin.ac.uk>
457) and was partly supported by the University of the Philippines Diliman Natural Sciences Research Institute
458 (NSRI), under the project entitled "*Investigating the effects of past and future changes in climate on a collection*
459 *of Philippine Super Typhoons and their flooding potential from the last 10 years (2012 – 2022) using a convection-*
460 *permitting regional climate model*" (ESM-24-1-01).

461

462 **Author Contributions**

463 RJD designed the study and prepared the first manuscript draft. All co-authors provided input, interpretation, and
464 revisions leading to the final paper.

465 **Conflicts of Interest**

466 I declare that the authors have no competing interests as defined by Copernicus Publications, or other interests
467 that might be perceived to influence the results and/or discussion reported in this paper

468



469 **Ethics approval/declarations (include appropriate approvals or waivers)**

470 *Not applicable*

471

472 **Consent to participate (include appropriate statements)**

473 *Not applicable*

474

475 **Consent for publication (include appropriate statements)**

476 *Not applicable*

477

478 **Data and Code Availability**

479 Simulation outputs are hosted on the JASMIN platform. The WRF model (Skamarock et al., 2008) and TRACK
480 tool (Hodges, 1995) were used. Data processing and figures were produced with CF-python and CF-plot and are
481 available from <https://www.ncas-cms.github.io/cf-python/>. Code for the WRF model is available at
482 <http://www.www2.mmm.ucar.edu/wrf/users/downloads.html>. WPS geographical input data are available from
483 https://www.www2.mmm.ucar.edu/wrf/users/download/get_sources_wps_geog.html#mandatory. The codes and
484 simulation data are available upon request to the corresponding author.

485

486

487 **References**

488

489 Allen, M. R., & Ingram, W. J. (2002). Constraints on future changes in climate and the hydrologic
490 cycle. *Nature*, 419(6903), 224-232.

491 Alvey, G. R. III, Zawislak, J., & Zipser, E. (2015). Precipitation properties observed during tropical cyclone
492 intensity change. *Monthly Weather Review*, 143(11), 4476–4492. [https://doi.org/10.1175/MWR-D-15-](https://doi.org/10.1175/MWR-D-15-0065.1)
493 0065.1

494 Bagtasa, G. (2017): Contribution of Tropical Cyclones to Precipitation in the Philippines. *Journal of Climate*. Vol
495 30. pp. 3621-3633. <http://dx.doi.org/10.1175/JCLI-D-16-0150.1>

496 Bagtasa, G. (2021): Analog forecasting of tropical cyclone precipitation in the Philippines, *J. Weather and Climate*
497 Extremes, 32, <https://doi.org/10.1016/j.wace.2021.100323>

498 Bagtasa, G. (2022). Variability of tropical cyclone precipitation volume in the Philippines. *International Journal*
499 *of Climatology*, 1– 11. <https://doi.org/10.1002/joc.7573>

500 Bhatia, K., Vecchi, G., Murakami, H., Underwood, S. & Kossin, J. Projected response of tropical cyclone intensity
501 and intensification in a global climate model. *J. Clim.* 31, 8281–8303 (2018).

502 Cha, E. J., Knutson, T. R., Lee, T. C., Ying, M., & Nakaegawa, T. (2020). Third assessment on impacts of climate
503 change on tropical cyclones in the Typhoon Committee Region–Part II: Future projections. *Tropical*
504 *Cyclone Research and Review*, 9(2), 75-86. <https://doi.org/10.1016/j.tccr.2020.04.005>

505 Cinco, T. A., de Guzman, R. G., Ortiz, A. M. D., Delfino, R. J. P., Lasco, R. D., Hilario, F. D., and Ares, E. D.
506 (2016). Observed trends and impacts of tropical cyclones in the Philippines. *International Journal of*
507 *Climatology*, 36(14). <https://doi.org/10.1002/joc.4659>



- 508 Cruz, F. T., Tacan, F. P., Uy, N. T. P., & Santillan, J. R. (2020). Topographical effects on precipitation distribution
509 during typhoons in the Philippines. *Natural Hazards*, 103(1), 1003-1020.
- 510 Da Silva, N.A., Haerter, J.O. Super-Clausius–Clapeyron scaling of extreme precipitation explained by shift from
511 stratiform to convective rain type. *Nat. Geosci.* 18, 382–388 (2025). [https://doi.org/10.1038/s41561-025-](https://doi.org/10.1038/s41561-025-01686-4)
512 [01686-4](https://doi.org/10.1038/s41561-025-01686-4)
- 513 DeMaria, M., Mainelli, M., Shay, L. K., Knaff, J. A., & Kaplan, J. (2005). Further improvement to the Statistical
514 Hurricane Intensity Prediction Scheme (SHIPS). *Weather and Forecasting*, 20(4), 531–543.
515 <https://doi.org/10.1175/WAF862.1>
- 516 Delfino, R.J.P., Bagtasa, G., Hodges, K., and Vidale, P.L.V. (2022). Sensitivity of simulating Typhoon Haiyan
517 (2013) using WRF: the role of cumulus convection, surface flux parameterizations, spectral nudging and
518 initial and boundary conditions. *Natural Hazards and Earth System Sciences Journal*.
519 <https://doi.org/10.5194/nhess-22-3285-2022>
- 520 Delfino, R.J.P., Vidale, P.L., Bagtasa, G., and Hodges, K. (2023). Response of damaging tropical cyclone events
521 in the Philippines to climate forcings from selected CMIP6 models using the pseudo global warming
522 technique. *Climate Dynamics*. <https://doi.org/10.1007/s00382-023-06742-6>
- 523 Delfino, R.J.P., Hodges, K., Vidale, P.L., and Bagtasa, G., and (2024). Sensitivity of Philippine historically
524 damaging tropical cyclone events to surface and atmospheric temperature forcings. *Regional Studies in*
525 *Marine Science*. <https://doi.org/10.1016/j.rsma.2024.103595>
- 526 Emanuel, K. (2005). Increasing destructiveness of tropical cyclones over the past 30 years. *Nature*, 436(7051),
527 686-688.
- 528 Emanuel, K. A. (1987). The dependence of hurricane intensity on climate. *Nature*, 326(6112), 483-485.
- 529 Emanuel, K. A. (1986). An air-sea interaction theory for tropical cyclones. Part I: Steady state maintenance, J.
530 *Atmos. Sci.*, 43, 585–604.
- 531 Held, Isaac M., and Brian J. Soden. "Robust responses of the hydrological cycle to global warming." *Journal of*
532 *climate* 19.21 (2006): 5686-5699.
- 533 Hendricks, E. A. M. S., Peng, B. F., & Li, T. (2010). Quantifying environmental control on tropical cyclone
534 intensity change. *Monthly Weather Review*, 138(8), 3243–3271.
535 <https://doi.org/10.1175/2010MWR3185.1>
- 536 Huprikar, A. S., Stansfield, A. M., & Reed, K. A. (2023). A storyline analysis of Hurricane Irma's precipitation
537 under various levels of climate warming. *Environmental Research Letters*, 19(1), 014004.
- 538 Jiang, H., & Ramirez, E. M. (2013). Necessary conditions for tropical cyclone rapid intensification as derived
539 from 11 years of TRMM data. *Journal of Climate*, 26(17), 6459–6470. [https://doi.org/10.1175/JCLI-D-12-](https://doi.org/10.1175/JCLI-D-12-00432.1)
540 [00432.1](https://doi.org/10.1175/JCLI-D-12-00432.1)
- 541 Kaplan, J., DeMaria, M., & Knaff, J. A. (2010). A revised tropical cyclone rapid intensification index for the
542 Atlantic and eastern North Pacific basins. *Weather and Forecasting*, 25(1), 220–241.
543 <https://doi.org/10.1175/2009WAF2222280.1>
- 544 Kaplan, J., Rozoff, C. M., DeMaria, M., Sampson, C. R., Kossin, J. P., Velden, C. S., ... Dostalek, J. F. (2015).
545 Evaluating environmental impacts on tropical cyclone rapid intensification predictability utilizing
546 statistical models. *Weather and Forecasting*, 30(5), 1374–1396. <https://doi.org/10.1175/WAF-D-15-0032.1>



- 547 Knutson, T. R. et al. Global projections of intense tropical cyclone activity for the late twenty-first century from
548 dynamical downscaling of CMIP5/RCP4.5 scenarios. *J. Clim.* 28, 7203–7224 (2015).
- 549 Knutson, T. R., McBride, J. L., Chan, J., Emanuel, K., Holland, G., Landsea, C., ... & Sugi, M. (2010). Tropical
550 cyclones and climate change. *Nature Geoscience*, 3(3), 157-163.
- 551 Knutson, T. R., McBride, J. L., Chan, J., Emanuel, K., Holland, G., Landsea, C., ... & Sugi, M. (2008). Tropical
552 cyclones and climate change. *Nature Geoscience*, 1(3), 157-163.
- 553 Kossin, J. P., Emanuel, K. A., & Vecchi, G. A. (2017). The poleward migration of the location of tropical cyclone
554 maximum intensity. *Nature*, 509(7500), 349-352.
- 555 Lau, W. K. M. & Zhou, Y. P. Observed recent trends in tropical cyclone precipitation over the North Atlantic and
556 the North Pacific. *J. Geophys. Res.* 117, D03104 (2012).
- 557 Lenderink, G., R. Barbero, J. M. Loriaux, and H. J. Fowler, 2017: Super-Clausius–Clapeyron Scaling of Extreme
558 Hourly Convective Precipitation and Its Relation to Large-Scale Atmospheric Conditions. *J. Climate*, **30**,
559 6037–6052, <https://doi.org/10.1175/JCLI-D-16-0808.1>.
- 560 Liu, M., Vecchi, G.A., Smith, J.A. et al. Causes of large projected increases in hurricane precipitation rates with
561 global warming. *npj Clim Atmos Sci* 2, 38 (2019). <https://doi.org/10.1038/s41612-019-0095-3>
- 562 Macalalad R, Delfino RJP, Badilla RA, Paat SF and G Bagtasa (2023). Role of Historical Warming on the Extreme
563 Flooding Event Due to Typhoon Vamco (Ulysses) 2020 in the Philippines. *Philipp J Sci* 152(S1): 197–
564 212. [https://philjournalsci.dost.gov.ph/publication/special-issues/meteorology/121-vol-152-no-s1-
565 meteorology/1973-role-of-historical-warming-on-the-extreme-flooding-event-due-to-typhoon-vamco-
566 ulysses-2020-in-the-philippines](https://philjournalsci.dost.gov.ph/publication/special-issues/meteorology/121-vol-152-no-s1-meteorology/1973-role-of-historical-warming-on-the-extreme-flooding-event-due-to-typhoon-vamco-ulysses-2020-in-the-philippines)
- 567 Montgomery, Michael T., John Persing, and Roger K. Smith. "Putting to rest WISHE-ful misconceptions for
568 tropical cyclone intensification." *Journal of Advances in Modeling Earth Systems* 7, no. 1 (2015): 92-109.
- 569 O'Gorman, P. A. (2020). Precipitation extremes in a warming climate. *Annual Review of Climate Science*, 1, 41-
570 63.
- 571 Pendergrass A G and Hartmann D L 2014 Two modes of change of the distribution of rain *J. Clim.* 27 8357–71
- 572 Rotunno, R., and K. A. Emanuel (1987), An air-sea interaction theory for tropical cyclones. Part II: Evolutionary
573 study using a nonhydrostatic axisymmetric numerical model, *J. Atmos. Sci.*, 44, 542–561.
- 574 Ruan, Z., & Wu, Q. (2018). Precipitation, convective clouds, and their connections with tropical cyclone intensity
575 and intensity change. *Geophysical Research Letters*, 45(2), 1098-1105.
- 576 Shi, X., Liu, Y., Chen, J. et al. Escalating tropical cyclone precipitation extremes and landslide hazards in South
577 China under Global Warming. *npj Clim Atmos Sci* 7, 107 (2024). [https://doi.org/10.1038/s41612-024-
578 00654-w](https://doi.org/10.1038/s41612-024-00654-w)
- 579 Trenberth, K. E., Dai, A., Rasmussen, R. M., & Parsons, D. B. (2003). The changing character of precipitation.
580 *Bulletin of the American Meteorological Society*, 84(9), 1205-1217.
- 581 Stansfield, A.M., Reed, K.A. Global tropical cyclone precipitation scaling with sea surface temperature. *npj Clim*
582 *Atmos Sci* **6**, 60 (2023). <https://doi.org/10.1038/s41612-023-00391-6>
- 583 Sun, Ying, et al. "How often will it rain?." *Journal of Climate* 20.19 (2007): 4801-4818.
- 584 Tao, C., & Jiang, H. (2015). Distributions of shallow to very deep precipitation-convection in rapidly intensifying
585 tropical cyclones. *Journal of Climate*, 28(22), 8791–8824. <https://doi.org/10.1175/JCLI-D-14-00448.1>



- 586 Tierra, M.C.M. and Bagtasa, G., (2023). Identifying the rapid intensification of tropical cyclones using the
587 Himawari-8 satellite and their impacts in the Philippines. *International Journal of Climatology*, 43(1), pp.1-
588 16.
- 589 Trenberth, K. E., Zhang, Y., & Fasullo, J. T. (2007). Global warming and the hydrologic cycle. *Journal of Climate*,
590 20(17), 3589-3610.
- 591 Trenberth, K. E. (2009). Precipitation in a changing climate-more floods and droughts in the future. *Gewex*
592 *News*, 19(May 2009), 8-10.
- 593 Vecchi, G. A. et al. Tropical cyclone sensitivities to CO₂ doubling: roles of atmospheric resolution, synoptic
594 variability and background climate changes. *Clim. Dyn.* <https://doi.org/10.1007/s00382-019-04913-y>
595 (2019).
- 596 Vecchi, G. A., Soden, B. J., Wittenberg, A. T., Held, I. M., Leetmaa, A., & Harrison, M. J. (2008). Weakening of
597 tropical Pacific atmospheric circulation due to anthropogenic forcing. *Nature*, 441(7089), 73-76.
- 598 Wang, S., Nie, J., Evans, J. P., & Zhu, X. (2019). Super Clausius–Clapeyron scaling of extreme hourly convective
599 precipitation and its relation to large-scale atmospheric conditions. *Geophysical Research Letters*, 46(11),
600 6122-6131.
- 601 Yamada, Y., M. Satoh, M. Sugi, C. Kodama, A. T. Noda, M. Nakano, and T. Nasuno, 2017: Response of Tropical
602 Cyclone Activity and Structure to Global Warming in a High-Resolution Global Nonhydrostatic Model. *J.*
603 *Climate*, 30, 9703–9724, <https://doi.org/10.1175/JCLI-D-17-0068.1>.
- 604 Yoshida, K., Sugi, M., Mizuta, R., Murakami, H. & Ishii, M. Future changes in tropical cyclone activity in high-
605 resolution large-ensemble simulations. *Geophys. Res. Lett.* 44, 9910–9917 (2017).
- 606 Xi, D., Wang, S., & Lin, N. (2023). Analyzing relationships between tropical cyclone intensity and rain rate over
607 the ocean using numerical simulations. *Journal of Climate*, 36(1), 81-91. [https://doi.org/10.1175/JCLI-D-](https://doi.org/10.1175/JCLI-D-22-0141.1)
608 [22-0141.1](https://doi.org/10.1175/JCLI-D-22-0141.1)